

HUPD-9830  
December 1998  
Revised March 1999

**Two-point correlation function of high-redshift objects on a light-cone :  
Effect of the linear redshift-space distortion**

Hiroaki Nishioka and Kazuhiro Yamamoto

Department of Physics, Hiroshima University, Higashi-Hiroshima 739-8526, Japan

**ABSTRACT**

A theoretical formulation for the two-point correlation function on a light-cone is developed in the redshift space. On the basis of the previous work by Yamamoto & Suto (1999), in which a theoretical formula for the two-point correlation function on a light-cone has been developed in the real space, we extend it to the formula in the redshift space by taking the peculiar velocity of the sources into account. A simple expression for the two-point correlation function is derived. We briefly discuss QSO correlation functions on a light-cone adopting a simple model of the sources.

*Subject headings:* cosmology: theory - dark matter - large-scale structure of universe

## 1. Introduction

The clustering of high-redshift objects is one of the current topics in the fields of observational cosmology and astrophysics. The high-redshift objects of  $z \gtrsim 1$  are becoming fairly common, and evidences of the clustering nature of such cosmic objects are reported in the various observational bands, e.g., X-ray selected AGNs (Carrera et al. 1998), the FIRST survey (Cress et al. 1996; Magliocchetti et al. 1998), high-redshift galaxies (Steidel et al. 1998; Giavalisco et al. 1998), and QSO surveys (Croom & Shanks 1996; Boyle et al. 1998). The statistics of these high-redshift objects are becoming higher, and we will be able to discuss the clustering at a quantitative level precisely in near future. From a theoretical point of view, the most important subject is to clarify the physical process of the formation history of these objects. The standard theoretical framework for the cosmic structure formation is based on the cold dark matter (CDM) model with gaussian initial density fluctuations. The clustering nature of the high-redshift objects provides us with many kinds of tests for the theoretical models (e.g., Peacock 1998; Jing & Suto 1998).

When analyzing the clustering nature of the high-redshift objects at a quantitative level, we must take the light-cone effect into account properly. Namely, such cosmological observations are feasible only on the light-cone hypersurface defined by the current observer. And the effect of the time-evolution of the sources, i.e., the luminosity function, the clustering amplitude, and the bias, contaminates an observational data. Thus this light-cone effect is especially important to discuss the three-dimensional two-point correlation function of the high-redshift objects. Some aspects of the light-cone effect has been discussed (Matarrese et al. 1997; Matsubara, Suto, & Szapudi 1997; Nakamura, Matsubara, & Suto 1998; Laix & Starkman 1998). Recently one of the authors (K.Y.) & Suto developed a formulation for the two-point correlation function for the high-redshift objects defined on the light-cone hypersurface (Yamamoto & Suto 1999; hereafter Paper I). The expression for the two-point correlation function on the light-cone was derived in a rigorous manner starting from first principle corresponding to the conventional pair-count analysis. This investigation is very important because it gives a rigorous relation between an observational data processing and a theoretical prediction as to the two-point correlation function on a light-cone for the first time. However this investigation is restricted to the formula in the real space, though observational maps of the high-redshift objects are obtained in the redshift space.

It is well known that the peculiar velocity of sources distorts their distribution in the redshift space (e.g., Davis & Peebles 1983; Kaiser 1987; Hamilton 1997). And this effect has been discussed as a probe of cosmological density parameters (e.g., Szalay, Matsubara, & Landy 1998; Nakamura, Matsubara, & Suto 1998; Matsubara & Suto 1996; Hamilton & Culhane 1996; Heavens & Taylor 1995; Suto, et al. 1999). In the previous paper (Paper I) the effect of the redshift-space distortion due to the peculiar velocity of the sources is not taken into account because it was formulated in the real space. From a practical point of view, the formula in the redshift space must be developed. The purpose of the present paper is to develop such a theoretical formula for the two-point correlation function on a light-cone hypersurface by taking the redshift-space distortion due to the peculiar velocity into account.

The paper is organized as follows: In §2 we develop a formulation for the two-point correlation function on the light-cone hypersurface in the redshift space in order to incorporate the linear redshift-space distortion. The expression for the two-point correlation function is presented in a rather simple form by using appropriate approximations. The main result is equation (32). As a demonstration of the usefulness of our formalism, we apply the formula to QSO correlation functions adopting a simple model of source distribution and cosmological models. The validity of the plane-parallel, or distant observer, approximation, for the correlation function of high-redshift objects is also discussed. §4 is devoted to discussion and conclusion. Throughout this paper we use the units in which the light velocity  $c$  is unity.

## 2. Two-point correlation function in the redshift space

In this section we develop a theoretical formulation for the two-point correlation function on a light-cone hypersurface in the redshift space by taking the peculiar motion of sources into account. In the present paper, we focus on the spatially-flat Friedmann-Lemaitre universe, whose line element is expressed in terms of the conformal time  $\eta$  as

$$ds^2 = a^2(\eta) \left[ -d\eta^2 + d\chi^2 + \chi^2 d\Omega_{(2)}^2 \right]. \quad (1)$$

Here the scale factor is normalized to be unity at present, i.e.,  $a(\eta_0) = 1$ . The Friedmann equation is

$$\left( \frac{\dot{a}}{a} \right)^2 = H_0^2 \left( \frac{\Omega_0}{a} + a^2 \Omega_\Lambda \right), \quad (2)$$

where  $\Omega_\Lambda = 1 - \Omega_0$ , the dot denotes  $\eta$  differentiation, and  $H_0$  is the Hubble constant  $H_0 = 100h$  km/s/Mpc.

Since our fiducial observer is located at the origin of the coordinates ( $\eta = \eta_0$ ,  $\chi = 0$ ), an object at  $\chi$  and  $\eta$  on the light-cone hypersurface of the observer satisfies a simple relation  $\eta = \eta_0 - \chi$ . Then the (real-space) position of the source on the light-cone hypersurface is specified by  $(\chi, \vec{\gamma})$ , where  $\vec{\gamma}$  is a unit directional vector. In order to avoid confusion, we introduce the radial coordinate  $r$  instead of  $\chi$ , and we denote the metric of the three-dimensional real space on which the observable sources are distributed, as follows,

$$ds_{LC}^2 = dr^2 + r^2 d\Omega_{(2)}^2. \quad (3)$$

Denoting the comoving number density of observed objects at a conformal time  $\eta$  and at a position  $(\chi, \vec{\gamma})$  by  $n(\eta, \chi, \vec{\gamma})$ , then the corresponding number density projected onto the space (3) is obtained by

$$n^{LC}(r, \vec{\gamma}) = n(\eta, \chi, \vec{\gamma}) \Big|_{\eta \rightarrow \eta_0 - r, \chi \rightarrow r}. \quad (4)$$

Introducing the mean *observed* (comoving) number density  $n_0(\eta)$  at time  $\eta$  and the density fluctuation of luminous objects  $\Delta(\eta, \chi, \vec{\gamma})$ , we write

$$n(\eta, \chi, \vec{\gamma}) = n_0(\eta) [1 + \Delta(\eta, \chi, \vec{\gamma})], \quad (5)$$

then equation (4) is rewritten as

$$n^{\text{LC}}(r, \vec{\gamma}) = n_0(\eta) [1 + \Delta(\eta, \chi, \vec{\gamma})] \Big|_{\eta \rightarrow \eta_0 - r, \chi \rightarrow r}. \quad (6)$$

Note that the mean *observed* number density  $n_0(\eta)$  is different from the mean number density of the objects  $\bar{n}(\eta)$  at  $\eta$  by a factor of the selection function  $\phi(\eta)$  which depends on the luminosity function of the objects and thus the magnitude-limit of the survey, for instance:  $n_0(\eta) = \bar{n}(\eta)\phi(\eta)$ .

In the similar way, if we know the peculiar velocity field, the corresponding quantity projected onto the space (3) is obtained by

$$\vec{v}^{\text{LC}}(r, \vec{\gamma}) = \vec{v}_c(\eta, \chi, \vec{\gamma}) \Big|_{\eta \rightarrow \eta_0 - r, \chi \rightarrow r}, \quad (7)$$

where  $\vec{v}_c(\eta, \chi, \vec{\gamma})$  is the CDM velocity field. Here we assume that the peculiar velocity field of luminous objects agrees with the CDM velocity field.

In Appendix A we summarized equations for the linear perturbation theory in the CDM dominated universe. Thus the linearized CDM density perturbation can be solved completely. However, the evolution of the source density fluctuations can not be solved completely since the bias mechanism is not well understood at present unfortunately. Then we must assume a model for the bias which connects the CDM density perturbations and the source number density fluctuations. In the present paper we assume the scale-dependent bias model:

$$b(k; \eta) = \frac{\Delta_{klm}(\eta)}{\delta_{klm}^{(c)}(\eta)}, \quad (8)$$

where  $\Delta_{klm}(\eta)$  and  $\delta_{klm}^{(c)}(\eta)$  are the Fourier coefficients for the source number density fluctuation and the CDM density fluctuation, respectively (see also Appendix A).

The next task is to describe the relation between the real space and the redshift space, since we consider the distribution of sources in the redshift space. First we consider how the peculiar velocity of a source distorts the estimation of the distance to the source. Let us assume that a source at redshift  $z$  (at a position  $(r, \vec{\gamma})$  in the real space) is moving with a peculiar velocity  $\vec{v}$ . The observed photon frequency  $\nu_{\text{obs}}$  and the emitted photon frequency  $\nu_{\text{emit}}$  is related as

$$\nu_{\text{obs}} = \frac{\nu_{\text{emit}}}{1+z} (1 - \vec{\gamma} \cdot \vec{v}). \quad (9)$$

From this equation, we find the shift in the apparent redshift due to the peculiar velocity as

$$\delta z = (1+z)(\vec{\gamma} \cdot \vec{v}). \quad (10)$$

From the Friedmann equation (2), we have

$$\delta \eta = -\frac{1}{H_0} \frac{a^{3/2} \delta z}{\sqrt{\Omega_0 + \Omega_\Lambda a^3}}. \quad (11)$$

Combining equations (10) and (11), then we obtain the apparent shift in the comoving coordinate due to the peculiar velocity as

$$\delta r = -\delta\eta = \frac{\mathcal{Z}(\eta)}{H_0} \vec{\gamma} \cdot \vec{v} \Big|_{\eta \rightarrow \eta_0 - r, \chi \rightarrow r}, \quad (12)$$

where we defined

$$\mathcal{Z}(\eta) = \frac{a(\eta)^{1/2}}{\sqrt{\Omega_0 + \Omega_\Lambda a(\eta)^3}}. \quad (13)$$

We introduce the variable  $s$  to denote the radial coordinate in the redshift space. Then a position in the redshift space is specified by  $(s, \vec{\gamma})$ , while the real space is done by  $(r, \vec{\gamma})$ . The relation between the redshift position and the real position is

$$s = r + \delta r, \quad (14)$$

where  $\delta r$  is specified by equation (12). The conservation of the number of sources gives (Hamilton 1997)

$$n_s(s, \vec{\gamma}) s^2 ds d\Omega_{\vec{\gamma}} = n^{\text{LC}}(r, \vec{\gamma}) r^2 dr d\Omega_{\vec{\gamma}}, \quad (15)$$

where  $n_s(s, \vec{\gamma})$  denotes the number density in the redshift space and  $n^{\text{LC}}(r, \vec{\gamma})$  does the number density in the real space. These two equations (14) and (15) specify the relation between the redshift space and the real space.

Now let us consider the two-point correlation function in the redshift space. We start from the following ensemble estimator for the two-point correlation function:

$$\mathcal{X}_s(R) = \frac{1}{V^{\text{LC}}} \int \frac{d\Omega_{\hat{\mathbf{R}}}}{4\pi} \int ds_1 s_1^2 d\Omega_{\vec{\gamma}_1} \int ds_2 s_2^2 d\Omega_{\vec{\gamma}_2} n_s(s_1, \vec{\gamma}_1) n_s(s_2, \vec{\gamma}_2) \delta^{(3)}(\mathbf{s}_1 - \mathbf{s}_2 - \mathbf{R}), \quad (16)$$

where  $\mathbf{s}_1 = (s_1, \vec{\gamma}_1)$  and  $\mathbf{s}_2 = (s_2, \vec{\gamma}_2)$  and  $R = |\mathbf{R}|$ ,  $\hat{\mathbf{R}} = \mathbf{R}/R$ , and  $V^{\text{LC}}$  is the comoving survey volume of the data catalogue:

$$V^{\text{LC}} = \int_{s_{\min}}^{s_{\max}} s^2 ds \int d\Omega_{\vec{\gamma}} = \frac{4\pi}{3} (s_{\max}^3 - s_{\min}^3), \quad (17)$$

with  $s_{\max} = s(z_{\max})$  and  $s_{\min} = s(z_{\min})$  being the boundaries of the survey volume. Equation (16) is a natural extension of the ensemble estimator for the two-point correlation function in the redshift space (see also Paper I).

By using equations (14) and (15), we rewrite equation (16) in terms of the variables in the real space:

$$\begin{aligned} \mathcal{X}_s(R) = \frac{1}{V^{\text{LC}}} \int \frac{d\Omega_{\hat{\mathbf{R}}}}{4\pi} \int dr_1 r_1^2 d\Omega_{\vec{\gamma}_1} \int dr_2 r_2^2 d\Omega_{\vec{\gamma}_2} n^{\text{LC}}(r_1, \vec{\gamma}_1) n^{\text{LC}}(r_2, \vec{\gamma}_2) \\ \times \delta^{(3)}(\mathbf{x}_1 + \delta\mathbf{x}_1 - \mathbf{x}_2 - \delta\mathbf{x}_2 - \mathbf{R}), \end{aligned} \quad (18)$$

where  $\mathbf{x}_1 + \delta\mathbf{x}_1 = (r_1 + \delta r_1, \vec{\gamma}_1)$ ,  $\mathbf{x}_2 + \delta\mathbf{x}_2 = (r_2 + \delta r_2, \vec{\gamma}_2)$ , and  $\delta r_1$  and  $\delta r_2$  are given by (12). Then we approximate as

$$\delta^{(3)}(\mathbf{x}_1 + \delta\mathbf{x}_1 - \mathbf{x}_2 - \delta\mathbf{x}_2 - \mathbf{R}) \simeq \left(1 + \delta\mathbf{x}_1 \cdot \frac{\partial}{\partial\mathbf{x}_1}\right) \left(1 + \delta\mathbf{x}_2 \cdot \frac{\partial}{\partial\mathbf{x}_2}\right) \delta^{(3)}(\mathbf{x}_1 - \mathbf{x}_2 - \mathbf{R}), \quad (19)$$

where we can write  $\delta\mathbf{x} \cdot \partial/\partial\mathbf{x} = \delta r \partial/\partial r$  since only the radial component of  $\delta\mathbf{x}$  has a non-zero value. By using this approximation and equation (6) we derive the following equation from (18):

$$\begin{aligned} \mathcal{X}_s(R) &= \frac{1}{V^{\text{LC}}} \int \frac{d\Omega_{\hat{\mathbf{R}}}}{4\pi} \int dr_1 r_1^2 d\Omega_{\vec{\gamma}_1} \int dr_2 r_2^2 d\Omega_{\vec{\gamma}_2} n_0^{\text{LC}}(r_1) n_0^{\text{LC}}(r_2) \\ &\quad \times \prod_{i=1}^2 \left[ 1 + \Delta(r_i, \vec{\gamma}_i) + \delta r_i \frac{\partial}{\partial r_i} \right] \delta^{(3)}(\mathbf{x}_1 - \mathbf{x}_2 - \mathbf{R}), \end{aligned} \quad (20)$$

where we used the notations:

$$n_0^{\text{LC}}(r) = n_0(\eta) \big|_{\eta \rightarrow \eta_0 - r}, \quad \Delta(r, \vec{\gamma}) = \Delta(\eta, \chi, \vec{\gamma}) \big|_{\eta \rightarrow \eta_0 - r, \chi \rightarrow r}, \quad (21)$$

and  $\delta r_i$  is understood as

$$\delta r_i = \frac{\mathcal{Z}(\eta)}{H_0} \vec{\gamma} \cdot \vec{v} \big|_{\eta \rightarrow \eta_0 - r_i, \chi \rightarrow r_i}, \quad (22)$$

where  $i = 1, 2$ .

Next we consider the ensemble average of the ensemble estimator  $\mathcal{X}_s(R)$ . Since  $\delta r_1$  and  $\delta r_2$  are the order of linear perturbation, then the ensemble average is written as

$$\langle \mathcal{X}_s(R) \rangle = \mathcal{U}(R) + \mathcal{W}_s(R), \quad (23)$$

where

$$\mathcal{U}(R) = \frac{1}{V^{\text{LC}}} \int \frac{d\Omega_{\hat{\mathbf{R}}}}{4\pi} \int dr_1 r_1^2 \int d\Omega_{\vec{\gamma}_1} \int dr_2 r_2^2 \int d\Omega_{\vec{\gamma}_2} n_0^{\text{LC}}(r_1) n_0^{\text{LC}}(r_2) \delta^{(3)}(\mathbf{x}_1 - \mathbf{x}_2 - \mathbf{R}), \quad (24)$$

and

$$\begin{aligned} \mathcal{W}_s(R) &= \frac{1}{V^{\text{LC}}} \int \frac{d\Omega_{\hat{\mathbf{R}}}}{4\pi} \int dr_1 r_1^2 \int d\Omega_{\vec{\gamma}_1} \int dr_2 r_2^2 \int d\Omega_{\vec{\gamma}_2} n_0^{\text{LC}}(r_1) n_0^{\text{LC}}(r_2) \\ &\quad \times \left\langle \left( \Delta(r_1, \vec{\gamma}_1) + \delta r_1 \frac{\partial}{\partial r_1} \right) \left( \Delta(r_2, \vec{\gamma}_2) + \delta r_2 \frac{\partial}{\partial r_2} \right) \right\rangle \delta^{(3)}(\mathbf{x}_1 - \mathbf{x}_2 - \mathbf{R}). \end{aligned} \quad (25)$$

In Appendix B we presented the explicit calculations for  $\mathcal{W}_s(R)$ . According to the result, equation (25) reduces to the following form within the linear theory of perturbation:

$$\begin{aligned} \mathcal{W}_s(R) &= \frac{1}{V^{\text{LC}}} \frac{1}{\pi R} \int \int_{\mathcal{S}} dr_1 dr_2 r_1 r_2 n_0^{\text{LC}}(r_1) n_0^{\text{LC}}(r_2) D_1(\eta_0 - r_1) D_1(\eta_0 - r_2) \\ &\quad \times \int dk k^2 P(k) \prod_{i=1}^2 \left[ b(k; \eta_0 - r_i) - k^{-2} \mathcal{D}_{r_i} \right] j_0 \left( k \sqrt{r_1^2 + r_2^2 - 2r_1 r_2 \cos \theta} \right), \end{aligned} \quad (26)$$

where

$$\mathcal{D}_r = f(\eta_0 - r) \frac{\partial^2}{\partial r^2} + f(\eta_0 - r) \frac{d}{dr} \ln \left[ r^2 n_0^{\text{LC}}(r) D_1(\eta_0 - r) f(\eta_0 - r) \right] \frac{\partial}{\partial r}, \quad (27)$$

and  $P(k)$  is the CDM power spectrum at present,  $D_1(\eta)$  is the linear growth rate normalized to be unity at present,  $f(\eta)$  is defined as  $f(\eta) = d \ln D_1(\eta) / d \ln a(\eta)$ , and  $\cos \theta$  should be replaced by  $\cos \theta = (r_1^2 + r_2^2 - R^2) / 2r_1 r_2$  after operating the differentiations with respect to  $r_1$  and  $r_2$ .

Omitting the second term in the derivative (27), equation (26) reduces to the simple form in the case  $R \ll r_{\min}$  and  $R \ll r_{\max}$  (see Appendix B),

$$\begin{aligned} \mathcal{W}_s(R) &\simeq \frac{4\pi}{V^{\text{LC}}} \int_{r_{\min}}^{r_{\max}} dr r^2 n_0^{\text{LC}}(r)^2 \frac{1}{2\pi^2} \int k^2 dk P(k) \left[ b(k; \eta_0 - r) D_1(\eta_0 - r) \right]^2 \\ &\times \left[ 1 + \frac{2}{3} \beta(\eta_0 - r) + \frac{1}{5} \beta(\eta_0 - r)^2 \right] j_0(kR), \end{aligned} \quad (28)$$

where  $\beta(k; \eta)$  is defined by

$$\beta(k; \eta) = \frac{f(\eta)}{b(k; \eta)} = \frac{1}{b(k; \eta)} \frac{d \ln D_1(\eta)}{d \ln a(\eta)}, \quad (29)$$

and we assumed  $s_{\max} = r_{\max}$  ( $s_{\min} = r_{\min}$ ).

We can derive the following equation from a similar calculation in the above (see also Paper I):

$$\mathcal{U}(R) \simeq \frac{4\pi}{V^{\text{LC}}} \int_{r_{\min}}^{r_{\max}} r^2 dr n_0^{\text{LC}}(r)^2. \quad (30)$$

Following Paper I, we define the two-point correlation function on the light-cone hypersurface:

$$\xi_s^{\text{LC}}(R) = \frac{\langle \mathcal{X}_s(R) \rangle - \mathcal{U}(R)}{\mathcal{U}(R)} = \frac{\mathcal{W}_s(R)}{\mathcal{U}(R)}. \quad (31)$$

Substituting equations (28) and (30) into (31), we have

$$\begin{aligned} \xi_s^{\text{LC}}(R) &\simeq \left[ \int_{r_{\min}}^{r_{\max}} dr r^2 n_0^{\text{LC}}(r)^2 \right]^{-1} \int_{r_{\min}}^{r_{\max}} dr r^2 n_0^{\text{LC}}(r)^2 \\ &\times \frac{1}{2\pi^2} \int k^2 dk P(k) b(k; \eta_0 - r)^2 D_1(\eta_0 - r)^2 \\ &\times \left[ 1 + \frac{2}{3} \beta(\eta_0 - r) + \frac{1}{5} \beta(\eta_0 - r)^2 \right] j_0(kR). \end{aligned} \quad (32)$$

This is the final expression for the two-point correlation function on the light-cone hypersurface in which the linear redshift-space distortion is taken into account. Comparing this result with  $\xi_A^{\text{LC}}(R)$  in Paper I, the terms in proportion to  $\beta(k; \eta)$  are the new terms which represent the effect of the linear redshift-space distortion.

### 3. A Simple Demonstration

In this section we apply the formula developed in the previous section to QSO two-point correlation function. Evidence for the spatial correlation in the QSO-distribution is reported (Croom & Shanks 1996; Boyle et al. 1998), however, it seems difficult to draw definite cosmological conclusions from the comparison with the currently available data. Then we only demonstrate the usefulness of our formalism by calculating the QSO two-point correlation function based on a simplified model for the distribution and the bias model. As for the bias, we here consider the scale-independent bias model by Fry (1996):

$$b(\eta) = 1 + \frac{1}{D_1(\eta)}(b_0 - 1), \quad (33)$$

where  $b_0$  is a constant parameter. Note that the bias  $b(\eta)$  at high-redshift becomes larger as  $b_0$  becomes larger. Here we also assume that the sources are distributed in the range  $0.3 \leq z \leq 3$  with a constant number density, i.e.,  $n_0 = \text{const.}$  This model may be over-simplified, however, we have checked that the qualitative features have not been changed even when adopting more realistic models in Paper I.

In figures 1 and 2 we show the two-point correlation function  $\xi_s^{\text{LC}}(R)$  and other mass correlation functions for comparison. We show the case for the standard cold dark matter (SCDM) model in Fig. 1, in which we adopted  $\Omega_0 = 1$ ,  $\Omega_\Lambda = 0$ ,  $h = 0.5$ , and the CDM density power spectrum normalized as  $\sigma_8 = 0.56$  (Kitayama & Suto 1997). The case for the cosmological model with a cosmological constant ( $\Lambda$ CDM model) is shown in Fig.2, in which  $\Omega_0 = 0.3$ ,  $\Omega_\Lambda = 0.7$ ,  $h = 0.7$ ,  $\sigma_8 = 1.0$  are adopted. In each panel (a)-(c), the three lines show the correlation functions on a light-cone. The solid line shows  $\xi_s^{\text{LC}}(R)$  of equation (32). The dashed line shows the case when neglecting the effect of the redshift-space distortion by setting  $\beta = 0$  in (32). On the other hand, the panel (d) shows the linear and nonlinear mass two-point correlation functions defined on a constant time hypersurface  $z = 0, 1$ , and 2.

From these figures it is apparent that the larger bias at the high-redshift derives the larger amplitude of the correlation function on a light-cone. Furthermore the effect of the redshift-space distortion always amplifies the correlation function from comparing the solid line and the dashed line in the panels (a)-(c), as expected. However the relative difference between the solid line and the dashed line becomes smaller as the bias becomes large and more effective. This is an expected feature because  $\beta$ -factor becomes smaller as the bias becomes larger (see eq.[29]).

We have also calculated the correlation function by adopting the exact expression (B20) instead of (28). The difference is less than 1 % for  $R \lesssim 100h^{-1}\text{Mpc}$ , and is negligible. Thus the formula (32) is a well approximated formula, and is an useful expression for the correlation function for high-redshift objects. The expression (32) is easily understood in an intuitive manner. Namely, the linear power spectrum in the redshift space is amplified by  $(1 + \beta\mu_{\mathbf{k}})^2$  over its unredshifted counterpart  $P(k)$  in the plane-parallel approximation, where  $\beta$  is defined in the same way as (29) and  $\mu_{\mathbf{k}} = \vec{\gamma} \cdot \mathbf{k}/k$  (e.g., Kaiser 1987; Hamilton 1997). This formula leads that the



angle-averaged redshift power spectrum is amplified by the factor,  $(1 + 2\beta/3 + \beta^2/5)$ , over the unredshifted power spectrum. Thus (32) is the expected formula obtained by multiplying the factor,  $(1 + 2\beta/3 + \beta^2/5)$ , at each cosmological time over unredshifted counterpart  $P(k)$  in the correlation function in the real space. In this sense the formula (32) is based on the plane-parallel approximation.<sup>1</sup> And our investigation shows that the use of the plane-parallel approximation is valid for the (angle-averaged) correlation function of high-redshift objects on a light-cone.

As we plotted absolute values of the two-point correlation functions in Figs. 1 and 2, then we can regard that the solid line and the dashed line show the anti-correlation at the large separation  $R \gtrsim$  a few  $\times 10h^{-1}\text{Mpc}$  in the SCDM model (see Fig. 1). Equation (32) implies that the zero-point of the correlation function is invariant even when the redshift space distortion is taken into account, as long as the bias does not depend on the scale  $k$ . The critical correlation length, where the correlation changes to the anti-correlation, is given by

$$R = \frac{16.6h^{-1}\text{Mpc}}{\Omega_0 h \exp[-\Omega_b - \sqrt{2h}\Omega_0/\Omega_b]}, \quad (34)$$

where we assumed the Harrison-Zeldovich initial density power spectrum and used the fitting formula for the transfer function (Bardeen et.al 1986; Sugiyama 1995). This critical correlation length may be observed in the upcoming 2dF and SDSS QSO surveys, and may be tested for the cosmological models and the theoretical models of bias.

#### 4. Summary and Discussion

In this paper we have developed a theoretical formulation for the two-point correlation function for high-redshift objects on a light-cone in the redshift space. Our formula has been developed by extending the previous work (Paper I) to the formula in the redshift space. We have started our formulation from considering the ensemble estimator of the two-point correlation function in the redshift space, then we have calculated the ensemble average of the estimator. Thus our formula has been derived in a rigorous manner starting from first principle corresponding to the conventional pair-count analysis. The calculation was cumbersome, however, a rather simple expression (32) has been derived.

We have demonstrated the effect of the redshift-space distortion by showing the QSO two-point correlation function adopting a very simple model of the source distribution and the bias, though it seems premature to draw definite cosmological conclusions from comparison with currently available data. As discussed in the below, our model adopted in this paper may be oversimplified in order to compare with a real data sample. Nevertheless our investigation is instructive and we have shown how the redshift-space distortion affects the correlation function for

---

<sup>1</sup>We thank T. Matsubara for his comment that our formula reproduces the formula inspired from such a consideration based on the plane-parallel approximation.

high-redshift objects on a light-cone (section 3). Our investigation shows that the redshift-space distortion becomes a small effect for time-varying bias models which have large values at high-redshift. The validity of the plane-parallel approximation is also shown for the correlation function of high-redshift objects on a light-cone.

There remain uncertainties to make precise theoretical predictions. First we did not attempt to examine possible bias models other than the model by Fry (1996). However, theoretical investigations for the time and scale dependent bias are just beginning (Fry 1996; Mo & White 1996; Dekel & Lahav 1998; Tegmark & Peebles 1998; Taruya, Koyama & Soda 1998). Conversely, the clustering of the high-redshift objects will be a good tool to test the bias models. Second we did not consider the realistic model for the time-evolution of number density in calculating QSO two-point correlation function. As for this point finite solution will be obtained in upcoming 2dF and SDSS QSO surveys. Third we have only considered the linear theory of the density perturbations, and the nonlinear effect was not considered here. According to the previous work (Paper I), the non-linearity of the source density fluctuation becomes important only at small separation  $R \lesssim$  a few  $h^{-1}\text{Mpc}$  (see also panel (d) in Figs. 1 and 2). And the effect of the non-linearity seems to be negligible at the large separation. However, the nonlinear effect in the redshift space has not been well understood especially for high-redshift objects, it must be investigated in future work. Probably numerical approaches would be needed for that purpose.

## ACKNOWLEDGMENTS

We thank Y. Kojima, Y. Suto and T. T. Nakamura for useful discussions and comments. We thank T. Matsubara for his crucial comments on the earlier manuscript. This research was supported in part by the Grants-in-Aid by the Ministry of Education, Science, Sports and Culture of Japan (09740203).

## APPENDIX

### A. Review of the linear theory of the CDM density perturbations

In this Appendix we summarize equations for the linear theory of the CDM density perturbations and explain the notations which are used in the present paper. The linearized CDM density perturbation in the CDM dominated universe obeys the following equations:

$$\dot{\delta}_c + v_c^i|_i = 0, \quad (\text{A1})$$

$$\dot{v}_c^i + \frac{\dot{a}}{a}v_c^i + \Psi^{,i} = 0, \quad (\text{A2})$$

$$\Psi^{,i}|_i = 4\pi G\rho a^2\delta_c = \frac{3\Omega_0 H_0^2}{2a}\delta_c, \quad (\text{A3})$$

where  $\delta_c$  is the CDM density contrast,  $v_c^i$  is the CDM velocity field,  $\Psi$  is the gravitational potential, which follows the gravitational poisson equation (A3), and  $|_i$  denotes the covariant derivative on the three-dimensional space.

As we are interested in the scalar perturbation, we expand the CDM density contrast  $\delta_c$  and the velocity field  $v_c^i$  in terms of the scalar harmonics as follows (e.g., Kodama & Sasaki 1984):

$$\delta_c(\eta, \chi, \vec{\gamma}) = \int_0^\infty dk \sum_{l,m} \delta_{klm}^{(c)}(\eta) \mathcal{Y}_{klm}(\chi, \vec{\gamma}), \quad (\text{A4})$$

$$v_c^i(\eta, \chi, \vec{\gamma}) = \int_0^\infty dk \sum_{l,m} v_{klm}(\eta) \mathcal{Y}_{klm}^i(\chi, \vec{\gamma}), \quad (\text{A5})$$

where  $\mathcal{Y}_{klm}$  is the normalized scalar harmonics:

$$\mathcal{Y}_{klm}(\chi, \vec{\gamma}) = X_k^l(\chi) Y_{lm}(\Omega_{\vec{\gamma}}), \quad (\text{A6})$$

with

$$X_k^l(\chi) = \sqrt{\frac{2}{\pi}} k j_l(k\chi), \quad (\text{A7})$$

$Y_{lm}(\Omega_{\vec{\gamma}})$  and  $j_l(x)$  are the spherical harmonics and the spherical Bessel function, respectively,  $k$  denotes the eigenvalue of the eigen-equation:  $\mathcal{Y}_{klm}^i|_i = -k^2 \mathcal{Y}_{klm}$ , and  $\mathcal{Y}_{klm}^i$  is defined as

$$\mathcal{Y}_{klm}^i(\chi, \vec{\gamma}) = -\frac{1}{k} \mathcal{Y}_{klm}(\chi, \vec{\gamma})^i. \quad (\text{A8})$$

From the linearized perturbation equations (A1)–(A3), we have

$$\dot{\delta}_{klm}^{(c)} + k v_{klm} = 0, \quad (\text{A9})$$

$$\dot{v}_{klm} + \frac{\dot{a}}{a} v_{klm} - k \Psi_{klm} = 0, \quad (\text{A10})$$

$$k^2 \Psi_{klm} = -\frac{3\Omega_0 H_0^2}{2a} \delta_{klm}^{(c)}, \quad (\text{A11})$$

where  $\Psi_{klm}$  is the Fourier coefficient defined in the same way as (A4). Combining these equations, we have

$$\ddot{\delta}_{klm}^{(c)} + \frac{\dot{a}}{a}\dot{\delta}_{klm}^{(c)} - \frac{3}{2}\frac{\Omega_0 H_0^2}{a}\delta_{klm}^{(c)} = 0. \quad (\text{A12})$$

In the Friedmann-Lemaitre universe, the growing mode solution is well known:

$$\delta_{klm}^{(c)}(\eta) = \delta_{klm}^{(c)}(\eta_0)D_1(a), \quad (\text{A13})$$

with

$$D_1(a) = A\sqrt{\frac{\Omega_0}{a^3} + 1 - \Omega_0} \int_0^a da' \left( \frac{a'}{\Omega_0 + a'^3(1 - \Omega_0)} \right)^{3/2}. \quad (\text{A14})$$

Here  $A$  is a constant to be determined so that  $D_1$  is unity at present. From equations (A9) and (A5), we finally have

$$v_c^i(\eta, \chi, \vec{\gamma}) = \int_0^\infty dk \sum_{l,m} \frac{\dot{\delta}_{klm}^{(c)}(\eta)}{k^2} \mathcal{Y}_{klm}(\chi, \vec{\gamma})^i. \quad (\text{A15})$$

## B. Calculation of $\mathcal{W}_s(R)$

In this Appendix we present an explicit calculation of  $\mathcal{W}_s(R)$ :

$$\begin{aligned} \mathcal{W}_s(R) &= \frac{1}{V_{\text{LC}}} \int \frac{d\Omega_{\hat{\mathbf{R}}}}{4\pi} \int dr_1 r_1^2 \int d\Omega_{\vec{\gamma}_1} \int dr_2 r_2^2 \int d\Omega_{\vec{\gamma}_2} n_0^{\text{LC}}(r_1) n_0^{\text{LC}}(r_2) \\ &\times \left\langle \left( \Delta(r_1, \vec{\gamma}_1) + \delta r_1 \frac{\partial}{\partial r_1} \right) \left( \Delta(r_2, \vec{\gamma}_2) + \delta r_2 \frac{\partial}{\partial r_2} \right) \right\rangle \delta^{(3)}(\mathbf{x}_1 - \mathbf{x}_2 - \mathbf{R}). \end{aligned} \quad (\text{B1})$$

Here  $\Delta(r, \vec{\gamma})$  and  $\delta r(r, \vec{\gamma})$  are explicitly written as

$$\Delta(r, \vec{\gamma}) = \int_0^\infty dk \sum_{l,m} \delta_{klm}^{(c)}(\eta_0) b(k; \eta_0 - r) D_1(\eta_0 - r) \mathcal{Y}_{klm}(r, \vec{\gamma}), \quad (\text{B2})$$

$$\begin{aligned} \delta r(r, \vec{\gamma}) &= \frac{\mathcal{Z}(\eta_0 - r)}{H_0} v_c^r(\eta_0 - r, r, \vec{\gamma}) \\ &= \int_0^\infty dk \sum_{l,m} \delta_{klm}^{(c)}(\eta_0) f(\eta_0 - r) D_1(\eta_0 - r) k^{-2} \mathcal{Y}_{klm}(r, \vec{\gamma})^r, \end{aligned} \quad (\text{B3})$$

where we defined

$$f(\eta) = \frac{\mathcal{Z}(\eta)}{H_0} \frac{\partial D_1(\eta)}{\partial \eta} \frac{1}{D_1(\eta)} = \frac{d \ln D_1(\eta)}{d \ln a(\eta)}, \quad (\text{B4})$$

and we used equations (2), (12), (8), (A13), and (A15). Substituting equations (B2) and (B3) into equation (B1), we obtain

$$\mathcal{W}_s(R) = \frac{1}{V_{\text{LC}}} \int \frac{d\Omega_{\hat{\mathbf{R}}}}{4\pi} \int dr_1 r_1^2 \int d\Omega_{\vec{\gamma}_1} \int dr_2 r_2^2 \int d\Omega_{\vec{\gamma}_2}$$

$$\begin{aligned}
& \times n_0^{\text{LC}}(r_1)n_0^{\text{LC}}(r_2)D_1(\eta_0 - r_1)D_1(\eta_0 - r_2) \\
& \times \int dk_1 \sum_{l_1, m_1} \int dk_2 \sum_{l_2, m_2} \langle \delta_{k_1 l_1 m_1}^{(c)}(\eta_0) \delta_{k_2 l_2 m_2}^{(c)*}(\eta_0) \rangle Y_{l_1 m_1}(\Omega_{\vec{\gamma}_1}) Y_{l_2 m_2}^*(\Omega_{\vec{\gamma}_2}) \\
& \times \prod_{i=1}^2 \left[ b(k_i; \eta_0 - r_i) X_{k_i}^{l_i}(r_i) + f(\eta_0 - r_i) k_i^{-2} X_{k_i}^{l_i}(r_i)^{|r_i} \frac{\partial}{\partial r_i} \right] \delta^{(3)}(\mathbf{x}_1 - \mathbf{x}_2 - \mathbf{R}).
\end{aligned} \tag{B5}$$

In addition, we use the relations

$$\delta^{(3)}(\mathbf{x}_1 - \mathbf{x}_2 - \mathbf{R}) = \frac{1}{(2\pi)^3} \int d^3 \mathbf{k} e^{-i\mathbf{k} \cdot (\mathbf{x}_1 - \mathbf{x}_2 - \mathbf{R})}, \tag{B6}$$

$$e^{-i\mathbf{k} \cdot \mathbf{x}} = 4\pi \sum_l \sum_{m=-l}^l (-i)^l j_l(k|\mathbf{x}|) Y_{lm}(\Omega_{\hat{\mathbf{k}}}) Y_{lm}^*(\Omega_{\hat{\mathbf{x}}}), \tag{B7}$$

then equation (B5) becomes

$$\begin{aligned}
\mathcal{W}_s(R) &= \frac{1}{V_{\text{LC}}} \int \frac{d\Omega_{\hat{\mathbf{R}}}}{4\pi} \int dr_1 r_1^2 \int d\Omega_{\vec{\gamma}_1} \int dr_2 r_2^2 \int d\Omega_{\vec{\gamma}_2} \\
& \times n_0^{\text{LC}}(r_1)n_0^{\text{LC}}(r_2)D_1(\eta_0 - r_1)D_1(\eta_0 - r_2) \\
& \times \int dk_1 \sum_{l_1, m_1} \int dk_2 \sum_{l_2, m_2} \langle \delta_{k_1 l_1 m_1}^{(c)}(\eta_0) \delta_{k_2 l_2 m_2}^{(c)*}(\eta_0) \rangle Y_{l_1 m_1}(\Omega_{\vec{\gamma}_1}) Y_{l_2 m_2}^*(\Omega_{\vec{\gamma}_2}) \\
& \times \prod_{i=1}^2 \left[ b(k_i; \eta_0 - r_i) X_{k_i}^{l_i}(r_i) + f(\eta_0 - r_i) k_i^{-2} X_{k_i}^{l_i}(r_i)^{|r_i} \frac{\partial}{\partial r_i} \right] \\
& \times \frac{1}{(2\pi)^3} \int d^3 \mathbf{k} 4\pi \sum_{L_1 M_1} (-i)^{L_1} j_{L_1}(kr_1) Y_{L_1 M_1}(\Omega_{\hat{\mathbf{k}}}) Y_{L_1 M_1}^*(\Omega_{\vec{\gamma}_1}) \\
& \quad \times 4\pi \sum_{L_2 M_2} (i)^{L_2} j_{L_2}(kr_2) Y_{L_2 M_2}^*(\Omega_{\hat{\mathbf{k}}}) Y_{L_2 M_2}(\Omega_{\vec{\gamma}_2}) \\
& \quad \times 4\pi \sum_{L_3 M_3} (i)^{L_3} j_{L_3}(kR) Y_{L_3 M_3}^*(\Omega_{\hat{\mathbf{k}}}) Y_{L_3 M_3}(\Omega_{\hat{\mathbf{R}}}),
\end{aligned} \tag{B8}$$

where  $k = |\mathbf{k}|$  and  $\hat{\mathbf{k}} = \mathbf{k}/|\mathbf{k}|$ . Integrating over  $\Omega_{\vec{\gamma}_1}$ ,  $\Omega_{\vec{\gamma}_2}$  and  $\Omega_{\hat{\mathbf{R}}}$  yields

$$\begin{aligned}
\mathcal{W}_s(R) &= \frac{1}{V_{\text{LC}}} \int dr_1 r_1^2 \int dr_2 r_2^2 n_0^{\text{LC}}(r_1)n_0^{\text{LC}}(r_2)D_1(\eta_0 - r_1)D_1(\eta_0 - r_2) \\
& \times \int dk_1 \sum_{l_1, m_1} \int dk_2 \sum_{l_2, m_2} \langle \delta_{k_1 l_1 m_1}^{(c)}(\eta_0) \delta_{k_2 l_2 m_2}^{(c)*}(\eta_0) \rangle \\
& \times \prod_{i=1}^2 \left[ b(k_i; \eta_0 - r_i) X_{k_i}^{l_i}(r_i) + f(\eta_0 - r_i) k_i^{-2} X_{k_i}^{l_i}(r_i)^{|r_i} \frac{\partial}{\partial r_i} \right] \\
& \times \frac{(4\pi)^2}{(2\pi)^3} \int d^3 \mathbf{k} (-i)^{l_1 - l_2} j_{l_1}(kr_1) j_{l_2}(kr_2) j_0(kR) Y_{l_1 m_1}(\Omega_{\hat{\mathbf{k}}}) Y_{l_2 m_2}^*(\Omega_{\hat{\mathbf{k}}}).
\end{aligned} \tag{B9}$$

And the further integration over  $\Omega_{\mathbf{k}}$  gives

$$\begin{aligned}
\mathcal{W}_s(R) &= \frac{1}{\sqrt{\text{VLC}}} \int dr_1 r_1^2 \int dr_2 r_2^2 n_0^{\text{LC}}(r_1) n_0^{\text{LC}}(r_2) D_1(\eta_0 - r_1) D_1(\eta_0 - r_2) \\
&\times \int dk_1 \int dk_2 \sum_l (2l+1) P(k_1) \delta(k_1 - k_2) \\
&\times \prod_{i=1}^2 \left[ b(k_i; \eta_0 - r_i) X_{k_i}^l(r_i) + f(\eta_0 - r_i) k_i^{-2} X_{k_i}^l(r_i)^{r_i} \frac{\partial}{\partial r_i} \right] \\
&\times \frac{(4\pi)^2}{(2\pi)^3} \int dk k^2 j_l(kr_1) j_l(kr_2) j_0(kR), \tag{B10}
\end{aligned}$$

where we used the relation of the gaussian random field in the linear theory:

$$\left\langle \delta_{k_1 l_1 m_1}^{(c)}(\eta_0) \delta_{k_2 l_2 m_2}^{(c)*}(\eta_0) \right\rangle = P(k_1) \delta(k_1 - k_2) \delta_{l_1 l_2} \delta_{m_1 m_2}, \tag{B11}$$

and  $\delta_{l_1 l_2}$  and  $\delta_{m_1 m_2}$  are the Kronecker's delta. Integration by parts yields:

$$\begin{aligned}
\mathcal{W}_s(R) &= \frac{1}{\sqrt{\text{VLC}}} \int dr_1 r_1^2 \int dr_2 r_2^2 n_0^{\text{LC}}(r_1) n_0^{\text{LC}}(r_2) D_1(\eta_0 - r_1) D_1(\eta_0 - r_2) \\
&\times \int dk_1 k_1^2 P(k_1) \sum_l (2l+1) \frac{4}{\pi^2} \int dk k^2 j_l(kr_1) j_l(kr_2) j_0(kR) \\
&\times \prod_{i=1}^2 \left[ \left( b(k_i; \eta_0 - r_i) - k_i^{-2} \mathcal{D}_{r_i} \right) j_l(k_i r_i) \right], \tag{B12}
\end{aligned}$$

where we used (A7), and the operator  $\mathcal{D}_r$  is defined by equation (27). Here the boundary terms are omitted since we can show that the boundary terms are the higher order terms of  $\mathcal{O}(R/r_{\text{max}})$  or  $\mathcal{O}(R/r_{\text{min}})$ , which are negligible in the case  $R \ll r_{\text{min}}$  and  $R \ll r_{\text{max}}$ .

Noting the relation (e.g., Magnus et al. 1966):

$$\int dk k^2 j_l(kr_1) j_l(kr_2) j_0(kR) = \begin{cases} \frac{\pi}{4r_1 r_2 R} P_l \left( \frac{r_1^2 + r_2^2 - R^2}{2r_1 r_2} \right) & (|r_1 - r_2| < R < r_1 + r_2), \\ 0 & (R < |r_1 - r_2|, R > r_1 + r_2), \end{cases} \tag{B13}$$

we find

$$\begin{aligned}
\mathcal{W}_s(R) &= \frac{1}{\sqrt{\text{VLC}}} \frac{1}{\pi R} \int \int_{\mathcal{S}} dr_1 dr_2 r_1 r_2 n_0^{\text{LC}}(r_1) n_0^{\text{LC}}(r_2) D_1(\eta_0 - r_1) D_1(\eta_0 - r_2) \\
&\times \int dk_1 k_1^2 P(k_1) \sum_l (2l+1) P_l \left( \frac{r_1^2 + r_2^2 - R^2}{2r_1 r_2} \right) \\
&\times \prod_{i=1}^2 \left[ \left( b(k_i; \eta_0 - r_i) - k_i^{-2} \mathcal{D}_{r_i} \right) j_l(k_i r_i) \right], \tag{B14}
\end{aligned}$$

where  $\mathcal{S}$  denotes the region  $|r_1 - r_2| \leq R \leq r_1 + r_2$ .

By using the additional theorem for the spherical Bessel function:

$$\sum_l (2l+1) P_l(\cos \theta) j_l(kr_1) j_l(kr_2) = j_0\left(k\sqrt{r_1^2 + r_2^2 - 2r_1r_2 \cos \theta}\right), \quad (\text{B15})$$

we can write

$$\begin{aligned} \mathcal{W}_s(R) &= \frac{1}{V^{\text{LC}}} \frac{1}{\pi R} \int \int_{\mathcal{S}} dr_1 dr_2 r_1 r_2 n_0^{\text{LC}}(r_1) n_0^{\text{LC}}(r_2) D_1(\eta_0 - r_1) D_1(\eta_0 - r_2) \\ &\times \int dk k^2 P(k) \prod_{i=1}^2 \left[ b(k; \eta_0 - r_i) - k^{-2} \mathcal{D}_{r_i} \right] j_0\left(k\sqrt{r_1^2 + r_2^2 - 2r_1r_2 \cos \theta}\right), \end{aligned} \quad (\text{B16})$$

where  $\cos \theta$  is replaced by  $\cos \theta = (r_1^2 + r_2^2 - R^2)/2r_1r_2$  after operating the differentiations by  $r_1$  and  $r_2$ .

Introducing the notation  $z = \sqrt{r_1^2 + r_2^2 - 2r_1r_2 \cos \theta}$ , we can show the formulas:

$$k^{-2} \frac{\partial^2}{\partial r_1^2} j_0(kz) = \frac{j_2(kz)}{z^2} (r_1 - r_2 \cos \theta)^2 - \frac{j_1(kz)}{kz}, \quad (\text{B17})$$

$$k^{-2} \frac{\partial^2}{\partial r_2^2} j_0(kz) = \frac{j_2(kz)}{z^2} (r_2 - r_1 \cos \theta)^2 - \frac{j_1(kz)}{kz}, \quad (\text{B18})$$

and

$$\begin{aligned} k^{-4} \frac{\partial^2}{\partial r_1^2} \frac{\partial^2}{\partial r_2^2} j_0(kz) &= \frac{j_4(kz)}{z^4} (r_1 - r_2 \cos \theta)^2 (r_2 - r_1 \cos \theta)^2 - \frac{j_3(kz)}{kz^3} \left\{ (r_1 - r_2 \cos \theta)^2 \right. \\ &\quad \left. - 4 \cos \theta (r_1 - r_2 \cos \theta) (r_2 - r_1 \cos \theta) + (r_2 - r_1 \cos \theta)^2 \right\} \\ &\quad + \frac{j_2(kz)}{(kz)^2} (2 \cos^2 \theta + 1). \end{aligned} \quad (\text{B19})$$

Using these formulas and omitting the second term in the derivative, i.e.,  $\mathcal{D}_r \simeq f(\eta_0 - r) \partial^2 / \partial r^2$ , we have

$$\begin{aligned} \mathcal{W}_s(R) &\simeq \frac{1}{V^{\text{LC}}} \frac{1}{\pi R} \int \int_{\mathcal{S}} dr_1 dr_2 r_1 r_2 n_0^{\text{LC}}(r_1) n_0^{\text{LC}}(r_2) \\ &\times \int dk k^2 P(k) \prod_{j=1}^2 \left[ b(k; \eta_0 - r_j) D_1(\eta_0 - r_j) \right] \\ &\times \left[ j_0(kR) + \beta(k; \eta_0 - r_2) I(R; r_1, r_2) + \beta(k; \eta_0 - r_1) I(R; r_2, r_1) \right. \\ &\quad \left. + \beta(k; \eta_0 - r_1) \beta(k; \eta_0 - r_2) J(R; r_1, r_2) \right], \end{aligned} \quad (\text{B20})$$

where  $\beta(k; \eta)$  is defined by equation (29), and  $I(R; r_1, r_2)$  and  $J(R; r_1, r_2)$  are defined by

$$I(R; r_1, r_2) = \frac{j_1(kR)}{kR} - \frac{j_2(kR)}{R^2} \left\{ \frac{R^2 + r_2^2 - r_1^2}{2r_2} \right\}^2, \quad (\text{B21})$$

and

$$\begin{aligned}
 J(R; r_1, r_2) = & \frac{j_2(kR)}{(kR)^2} \left[ 2 \left\{ \frac{r_1^2 + r_2^2 - R^2}{2r_1 r_2} \right\}^2 + 1 \right] \\
 & + \frac{j_4(kR)}{R^4} \left\{ \frac{R^2 + r_1^2 - r_2^2}{2r_1} \right\}^2 \left\{ \frac{R^2 + r_2^2 - r_1^2}{2r_2} \right\}^2 \\
 & - \frac{j_3(kR)}{kR^3} \left[ \left\{ \frac{R^2 + r_1^2 - r_2^2}{2r_1} \right\}^2 + \left\{ \frac{R^2 + r_2^2 - r_1^2}{2r_2} \right\}^2 \right. \\
 & \quad \left. - \frac{R^2 + r_1^2 - r_2^2}{r_1} \frac{R^2 + r_2^2 - r_1^2}{r_2} \frac{r_1^2 + r_2^2 - R^2}{2r_1 r_2} \right], \tag{B22}
 \end{aligned}$$

respectively.

Since we are generally interested in the case of  $R \ll r_{\max}$ , we can use the approximation:

$$\int \int_{\mathcal{S}} dr_1 dr_2 \simeq \int_{r_{\min}}^{r_{\max}} dr_1 \int_{-R}^R dx, \tag{B23}$$

where we introduced  $x = r_2 - r_1$ . By expanding  $I(R; r_1, r_2)$  and  $J(R; r_1, r_2)$  in terms of  $x$ , we have

$$I(R; r_1, r_2) = \frac{j_1(kR)}{kR} - \frac{j_2(kR)}{R^2} x^2 \tag{B24}$$

$$J(R; r_1, r_2) = 3 \frac{j_2(kR)}{(kR)^2} - 6 \frac{j_3(kR)}{kR^3} x^2 + \frac{j_4(kR)}{R^4} x^4 \tag{B25}$$

Integration by  $x$  leads to the final expression:

$$\begin{aligned}
 \mathcal{W}_s(R) \simeq & \frac{4\pi}{V_{\text{LC}}} \int_{r_{\min}}^{r_{\max}} dr r^2 n_0^{\text{LC}}(r)^2 \frac{1}{2\pi^2} \int k^2 dk P(k) \left[ b(k; \eta_0 - r) D_1(\eta_0 - r) \right]^2 \\
 & \times \left[ 1 + \frac{2}{3} \beta(\eta_0 - r) + \frac{1}{5} \beta(\eta_0 - r)^2 \right] j_0(kR). \tag{B26}
 \end{aligned}$$



## REFERENCES

- Bardeen, J.M., Bond, J.R, Kaiser, N., & Szalay, A.S. 1986, *ApJ*, 304, 15
- Boyle, B.J., Croom, S.M., Smith, R.J., Shanks, T., Miller L., & Loaring, N. 1998, *Phil.Trans.R.Soc.Lond.A*, in press (astro-ph/9805140).
- Carrera, F.J. et al. 1998, *MNRAS*, 299, 229
- Cress, C.M., Helfand, D.J., Becker, R.H., Gregg, M.D., & White, R.L. 1996, *ApJ*, 473, 7
- Croom, S.M. & Shanks, T.1996, *MNRAS*, 281, 893
- Davis, M. & Peebles, P.J.E. 1983, *ApJ*, 267, 465
- Dekel, A. & Lahav, O. 1998, *ApJ*, submitted (astro-ph/9806193).
- de Laix, A. A. & Starkman, G. D. 1998, *MNRAS*, 299, 977
- Fry, J. N. 1996, *ApJ*, 461, L65
- Giavalisco, M., Steidel, C.C., Adelberger, K.L., Dickinson, M., Pettini, M., & Kellogg, M. 1998, *ApJ*, 503, 543
- Hamilton, A.J.S. 1997, to appear in the Proceedings of Ringberg Workshop on Large-Scale Structure, edited by Hamilton, D. (astro-ph/9708102).
- Hamilton, A.J.S. & Culhane, M. 1996, *MNRAS*, 278, 73
- Heavens, A.F. & Taylor, A.N. 1995, *MNRAS*, 275, 483
- Jing, Y.P., & Suto, Y. 1998, *ApJ*, 494, L5
- Kaiser, N. 1987, *MNRAS*, 227, 1
- Kitayama, T. & Suto, Y. 1997, *ApJ*, 490, 557
- Kodama, H. & Sasaki, M. 1984, *Prog. Theor. Phys. Supp.*, 78, 1
- Magliocchetti. M., Maddox, S.J., Lahav, O., & Wall, J.V. 1998, *MNRAS*, submitted (astro-ph/9806342).
- Matarrese, S., Coles, P., Lucchin, F., & Moscardini, L. 1997, *MNRAS*, 286, 115
- Matsubara, T. & Suto, Y. 1996, *ApJ*, 470, L1
- Matsubara, T. , Suto, Y., & Szapudi,I. 1997, *ApJ*, 491, L1
- Mo, H.J. & White, S.D.M. 1996, *MNRAS*, 282, 347
- Nakamura, T.T., Matsubara, T., & Suto, Y. 1998, *ApJ*, 494, 13
- Peacock, J.A. 1998, *Phil.Trans.R.Soc.Lond.A*, in press (astro-ph/9805208).
- Steidel, C.C., Adelberger, K.L., Dickinson, M., Giavalisco, M., Pettini, M., & Kellogg, M. 1998, *ApJ*, 492, 428
- Sugiyama, N. 1995, *ApJS*, 100, 281
- Suto, Y., Magira, H., Jing, Y.P., Matsubara, T., & Yamamoto, K. 1999, *Prog. of Theor. Phys. Suppl.*, in press (astro-ph/9901179).
- Szalay, A.S., Matsubara, T., & Landy, S.D. 1998, *ApJ*, 498, L1
- Taruya, A., Koyama, K., & Soda, J. 1998, *ApJ*, in press (astro-ph/9807005).

Tegmark, M. & Peebles, P.J.E. 1998, ApJ, 500, L79

Yamamoto, K. & Suto, Y. 1999, ApJ, in press (Paper I).

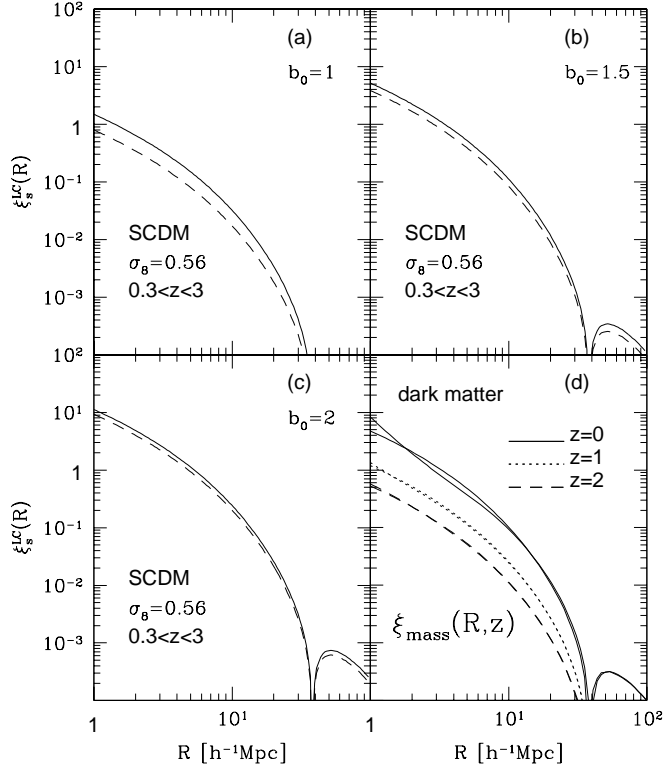


Fig. 1.— Absolute values of the two-point correlation function for QSO on a light-cone and the linear and nonlinear mass two-point correlation functions in the standard CDM model, where we adopted  $\Omega_0 = 1$ ,  $\Omega_\Lambda = 0$ ,  $h = 0.5$ , and the CDM density power spectrum normalized as  $\sigma_8 = 0.56$  (Kitayama & Suto 1997). The parameter  $b_0$  for the bias model are adopted as (a)  $b_0 = 1$ , (b)  $b_0 = 1.5$ , (c)  $b_0 = 2$ . Here we assumed that the sources are distributed in the range  $0.3 \leq z \leq 3$  with a constant number density. In each panel (a)-(c) the solid line shows our  $\xi_s^{LC}(R)$ , the dashed line does the case when the redshift-space distortion is neglected by setting  $\beta = 0$ , (d) linear (lower curves) and nonlinear (upper curves) mass correlation functions by Peacock & Dodds (1996) defined on constant-time hypersurfaces  $z = 0, 1$  and  $2$ .

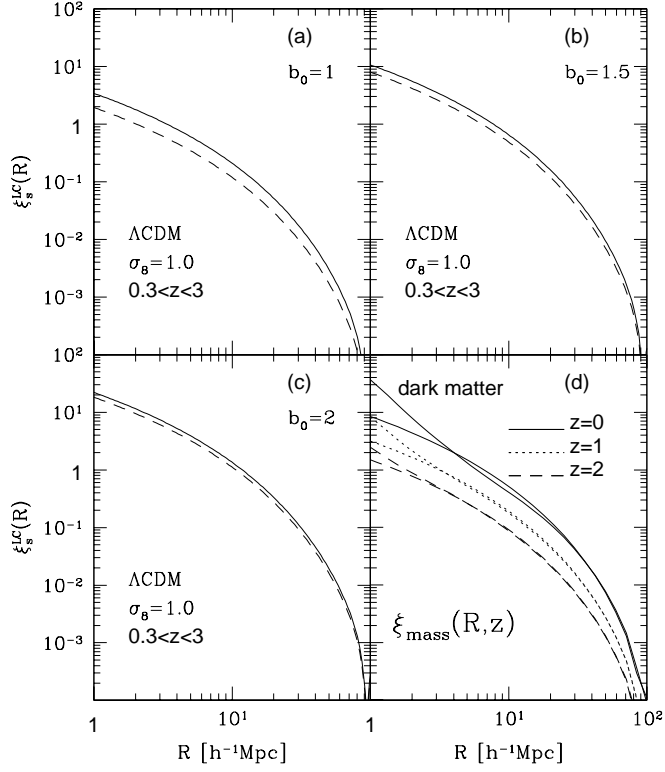


Fig. 2.— Same as Fig. 1 but for the  $\Lambda$ CDM model, in which we adopted  $\Omega_0 = 0.3$ ,  $\Omega_\Lambda = 0.7$ ,  $h = 0.7$ ,  $\sigma_8 = 1.0$ .